DOI: 10.1002/ejic.200900870

meta-Terphenyl Phosphaalkenes Bearing Electron-Donating and -Accepting Groups

Vittal B. Gudimetla,[a] Liqing Ma,[a] Marlena P. Washington,[a] John L. Payton,[a] M. Cather Simpson,[b] and John D. Protasiewicz*[a]

Keywords: Phosphorus / Phosphaalkenes / Solid-state structures / Electrochemistry

A set of *para*-substituted *meta*-terphenyl phosphaalkenes of the form 4-X-2,6-$Mes_2C_6H_2P$=C(H)C_6H_4-4-X′ (X = H, MeO or NMe_2; X′ = H, CN, or NO_2) have been synthesized to allow systematic studies of the impact of remote X and X′ substituents on the phosphaalkene unit. The new compounds were characterized by ^1H and ^{31}P NMR spectroscopy, UV/Vis absorption spectroscopy, single X-ray crystal structures (for four compounds) and by electrochemical studies. The introduction of remote groups (X′) on the less hindered phenyl ring generated more significant effects on the physical properties of the materials than did substituents (X) on the hindered *meta*-terphenyl rings. These effects were also explored by computational methods in order to assess the influence of substituents on structures and properties. The polarization of these molecules is less than that produced for analogous alkenes, as the phosphaalkenes bear sterically demanding groups that constrain the systems to adopt conformations that are less than ideal for maximum π-conjugation of the central π network

Introduction

Phosphaalkenes ($RP=CR'_2$) represent interesting main-group analogues of alkenes ($R_2C=CR'_2$).[1–9] As such, in many of the areas for which alkenes are either being used or studied for technological applications, parallel opportunities often exist for phosphaalkenes. For example, we and others have been developing conjugated polymers featuring phosphaalkene functionalities along the main chain.[10–15] Another set of materials that has captured much attention are nonlinear optical (NLO) active materials based upon alkenes.[16] Many of these promising materials feature alkenes are those that are polarized by the simultaneous presence of both electron-donating (ED) groups and electron-withdrawing (EW) groups. Like alkenes, phosphaalkenes are relatively non polar in the absence of strongly polarizing groups, due to the similar electronegativities of carbon [χ(C) = 2.5] and phosphorus [χ(P) = 2.2]. This slight difference, however, could accomodate contributions from resonance structures **ii** and **iii**.

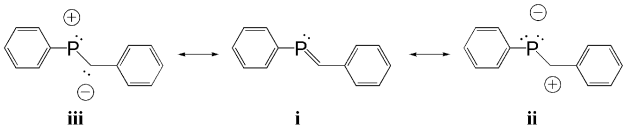

iii **i** **ii**

The effect of introducing polarizing functional groups on phosphaalkenes has received some preliminary investigation. For example, Bickelhaupt and colleagues performed a systematic analysis of the impact of varying remote *para*-X′-substituents on (*E*)-Mes*P=C(H)C_6H_4-4-X′ (Mes* = 2,4,6-$tBu_3C_6H_2$ **A**).[17] They concluded that the Mes*P=CH group acts as a weak electron donor on substituted benzene rings, much as with simple alkenes. In another pioneering study, Yoshifuji and colleagues successfully re-engineered the bulky Mes* to allow variation of the *para*-X-substituent on the bulky aryl group (**B**). For a series of fluorenylidene-(aryl)phosphanes, the UV/Vis spectroscopic data suggested that the X group influenced the phosphorus lone pair energetics significantly more than the energies of the π or π* orbitals.[18] These results can be rationalized by the fact the very sterically demanding Mes*-type ligands (as illustrated by **A** and **B**) and their *ortho*-*tert*-butyl groups cause the phenyl rings to be nearly orthogonal to the plane best suited for conjugation to the P=C π-bond. Thus the impact of remote substituents on the P=C π-bonds in systems such as **B** are expected to be diminished compared to those modified as in **A**. Yoshifuji and co-workers have also employed such functionalized ligands to introduce diarylamino groups into remote position of terphenyl ligands for the purpose of preparing multi-redox-active diphosphenes (**C**).[19,20]

In some cases, directly attaching electron-donating groups can even reverse the slight polarization of the P=C

[a] Department of Chemistry, Case Western Reserve University, 10900 Euclid Avenue, Cleveland, OH 44106, USA
E-mail: protasiewicz@case.edu
[b] Departments of Chemistry and Physics and The Dan Walls Centre for Pure and Applied Optics, The University of Auckland,
Auckland, New Zealand

Supporting information for this article is available on the WWW under http://dx.doi.org/10.1002/ejic.200900870.

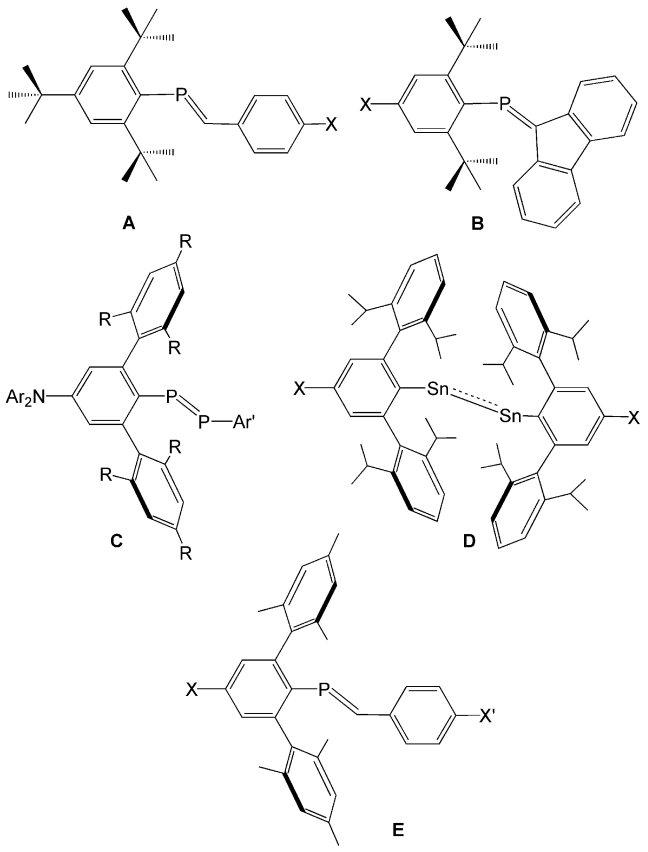

bond to create inversely polarized phosphaalkenes having very different chemistries.[21]

The addition of remote substituents can have important consequences for other main group multiply bonded compounds. For example, Power and co-workers have shown that for certain distannyne analogues (**D**), a change from X = H to X = $SiMe_3$ can have dramatic effects on Sn–Sn bond lengths, C–Sn–Sn bond angles, and even the orientation of the aryl rings with respect to the Ar–Sn–Sn–Ar torsional angles.[22]

The goal of our studies was to prepare a set of phosphaalkenes with varying degrees of polarization across the central P=C unit.

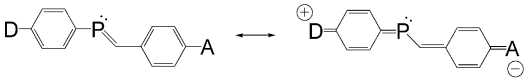

For the present study, analogues of the bulky 2,6-$Mes_2C_6H_3$ group (**E**) have been chosen. These terphenyl ligands can more readily access coplanar configurations better suited for π-conjugation across the whole system than the Mes*-type ligands. We have previously reported on the syntheses of both (*E*)-2,6-$Mes_2C_6H_3P{=}C(H)C_6H_4$-4-X′ (**E**, X = H; X′ = H, Cl, NO_2, OMe, NMe_2)[23] and (*E*)-4-Br-2,6-$Mes_2C_6H_2P{=}C(H)C_6H_4$-4-Br (**E**, X = X′ = Br)[24] systems. The latter material was also isolated in its *Z*-form, as the product of photoisomerization.[24]

Results and Discussion

Synthesis of Phosphaalkenes and Functionalized *meta*-Terphenyl Groups

Yoshifuji and co-workers demonstrated the utility of dihalo-substituted 2,6-dimesitylphenyl groups such as 4-I-2,6-$Mes_2C_6H_2I$ and 4-I-2,6-$Tip_2C_6H_2I$.[19,20] Our approach to the present terphenyls starts with the readily prepared related compound 4-Br-2,6-$Mes_2C_6H_2Br$ (**1**). Compound **1** can then be easily converted to 4-I-2,6-$Mes_2C_6H_2Br$ (**2**) as shown in Scheme 1.

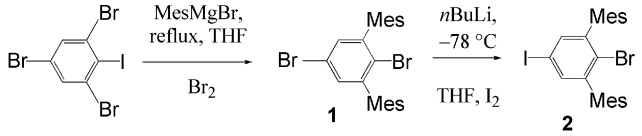

Scheme 1.

Compound **2** allows for the synthesis of the terphenyl bearing Me_2N (**5a**) and MeO (**5b**) substituents, as outlined in Scheme 2 and Scheme 3. A set of conventional transformations based on related syntheses were used with good success.[25–27]

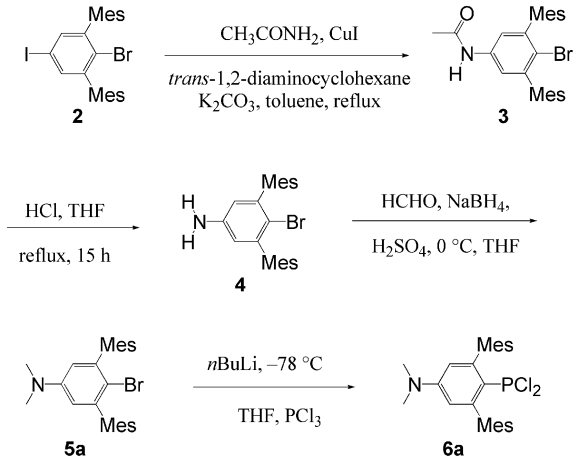

Scheme 2.

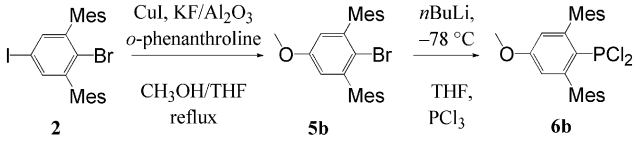

Scheme 3.

From **5a**,**b** the corresponding aryldichlorophosphanes 4-Me_2N-2,6-$Mes_2C_6H_2PCl_2$ (**6a**) and 4-CH_3O-2,6-$Mes_2C_6H_2PCl_2$ (**6b**) can be accessed in modest to good yields (30% and 50%, respectively). The reduced yields reflect, in part, the greater difficulty encountered in the purification of these materials. The ^{31}P NMR shifts for **6a** and **6b** located at δ = 163.7 and 160.7 ppm are close to the value of 160.1 ppm reported for the unsubstituted analogue 2,6-$Mes_2C_6H_3PCl_2$.

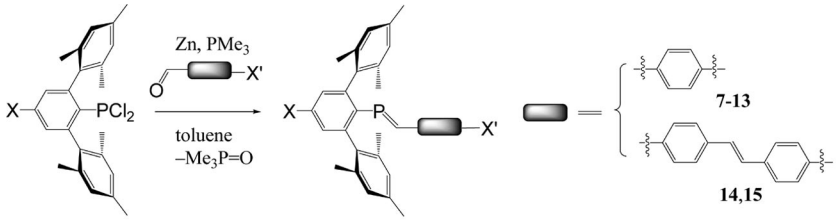

	X	X'	% Yield	^{31}P NMR ($CDCl_3$) (δ)	^{13}C NMR ($CDCl_3$) δ for P=C(H)Ar
7	H	H	76	241.9 (240.9*)	180.2 (J_{PC} = 35.0)
8	H	NO_2	43	268.4 (265.6*)	176.5 (J_{PC} = 36.4)
9	H	CN	46	263.5	177.0 (J_{PC} = 35.8)
10	MeO	CN	67	262.6	176.3 (J_{PC} = 35.2)
11	MeO	NO_2	35	267.0	176.2 (J_{PC} = 36.4)
12	MeO	H	47	240.7	180.1 (J_{PC} = 35.2)
13	Me_2N	H	40	242.5	178.4 (J_{PC} = 35.3)
14	H	NO_2	75	245.1	178.9 (J_{PC} = 35.6)
15	MeO	NO_2	71	245.7	178.6 (J_{PC} = 35.6)

* δ value for C_6D_6 solution.

Scheme 4.

While several routes have been reported for the synthesis of phosphaalkenes, we have found that for the synthesis of terphenyl-bearing phosphaalkenes the use of "phospha-Wittig" reagents of the form 2,6-$Mes_2C_6H_3P{=}PMe_3$ to be particularly convenient.[9,23] These reagents need not be isolated and they can be easily generated by the reduction of $ArPCl_2$ by Zn dust in the presence of PMe_3. Subsequent addition of aldehydes afford the corresponding phosphaalkenes in good yields. The phosphaalkenes **7**–**15** were prepared in this manner using commercially available aldehydes and (*E*)-4-(4-nitrostyryl)benzaldehyde (Scheme 4).

Examination of the ^{31}P NMR shift data for **8**–**15** shows that the presence of electron-withdrawing groups X′ (note **8**, **9**) leads to significant downfield shifts (ca. 23–25 ppm) relative to **7**. By comparison, a much smaller impact for the presence of X groups is noted (**12**, **13**) on ^{31}P NMR shifts (ca. 2 ppm) relative to **7** or to compounds that have non-hydrogen X′ groups. These findings can be rationalized by the tendency of the much larger aryl group to rotate so as to minimize unfavorable steric interactions, as in **E′** in Scheme 5. Thus, the ability of the remote substituents X to electronically communicate with the P=C functional group via π-conjugation through the aromatic rings are inhibited, relative to that of the X′ units on the less hindered aryl ring.

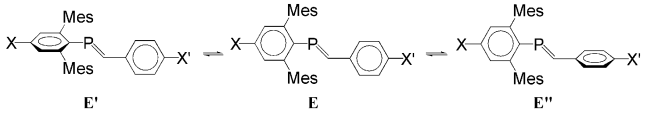

Scheme 5.

UV/Vis Absorption Data

The phosphaalkenes **7**–**15** vary in color from pale yellow to reddish orange. The intensity of the color is visibly higher for **14** and **15**. The UV/Vis absorption spectra of the phosphaalkenes **7**–**12** afford an opportunity to assess the relative impact of X and X′ substituents on these phosphaalkenes.

Figure 1 shows that electron-withdrawing groups are more effective at redshifting the π–π* transitions when they are substituted on the less sterically hindered phenyl ring. The absorption maxima of the X′ = NO_2 (**8**) and X′ = CN

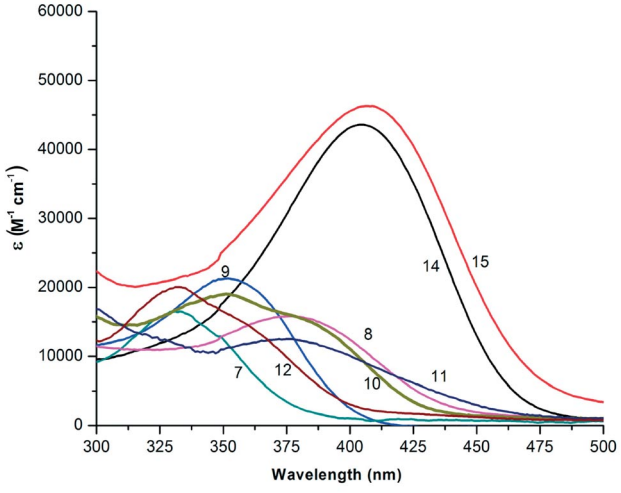

	λ_{max} (shoulder) nm	log ε
7	331 (340)	4.23
8	377	4.21
9	352	4.32
10	351	4.28
11	376 (380)	4.08
12	332 (355)	4.27
14*	402	4.65
15	409	4.66

* Insufficient amount of **13** available for analysis.

Figure 1. UV/Vis absorption spectra of phosphaalkenes in $CHCl_3$.

(**9**) are shifted relative to unsubstituted **7** by 46 and 21 nm, respectively. The introduction of an electron-donating methoxy group to the bulky *meta*-terphenyl unit had little influence on the π–π* transition, largely due to the weak π-delocalization of π electrons from this ligand to the rest of the molecule. This can be seen by comparing the absorption maxima for compounds **7** (331 nm) with **12** (332 nm), **9** (352 nm) with **10** (351 nm), and **14** (402 nm) with **15** (409 nm).

X-ray Crystallographic Studies

X-ray quality crystals of **8**, **9**, **10**, and **12** were obtained from their respective concentrated solutions of ethyl ether at –35 °C. The ORTEP representations and results of these structure determinations are shown in Figures 2 and 3, and the corresponding crystallographic data is given in Tables 1 and 2, respectively.

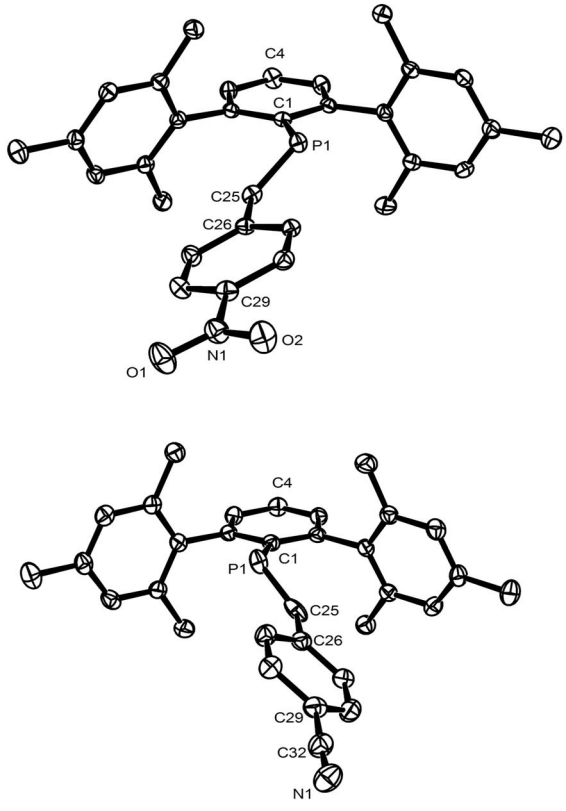

Figure 2. Single crystal X-ray crystallographic structures of (*E*)-2,6-$Mes_2C_6H_3P{=}C(H)C_6H_4$-4-$NO_2$ (**8**, top) and (*E*)-2,6-$Mes_2C_6H_3$-$P{=}C(H)C_6H_4$-4-CN (**9**, bottom) shown at the 50% thermal ellipsoid level (hydrogen atoms omitted for clarity).

All four structures are similar in that they feature comparable C–P–C bond angles ranging from 103.3–105.9°. The shorter P=C bond length for the structure of **9** is, however, suspect, for we recently uncovered a temperature dependent disorder of the phosphorus atoms in related *meta*-terphenyl diphosphenes, ArP=PAr, that can result in anomalously short P–P distances for data sets collected at room temperature.[28] The other P=C bond lengths vary from 1.649(4) to 1.672(1) Å. If the primary impact on the P=C bond lengths was controlled by resonance contributions, then one might expect the greatest P=C bond lengths to be observed for compound **10** having both electron-donating and withdrawing groups. These resonance structures, however, require that the participatory phenyl rings and the P=C unit all be coplanar to achieve maximal conjugation. The angles α_1 of the plane of the C–P=C–C atoms to those of each attached phenyl ring can be measured and compared (Table 2). For each molecule, α_1 is much greater than α_2, owing to the much larger attached phenyl ring. Figure 4 shows that compound **10** displays the maximum perturbation from a maximally conjugated conformation.

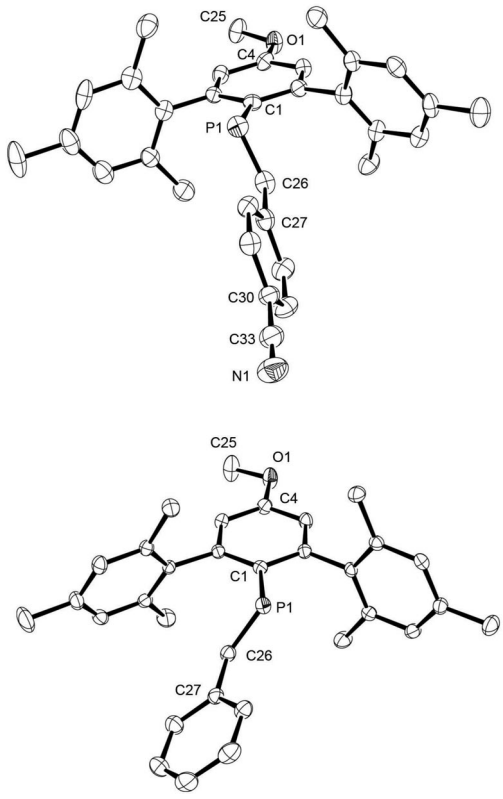

Figure 3. Single crystal X-ray crystallographic structures of (*E*)-4-CH_3O-2,6-$Mes_2C_6H_2P{=}C(H)C_6H_4$-4-CN (**10**, top) and (*E*)-4-CH_3O-2,6-$Mes_2C_6H_2P{=}C(H)C_6H_5$ (**12**, bottom) shown at the 50% thermal ellipsoid level (hydrogen atoms omitted for clarity).

This analysis, however, is subject to the unknown influence of packing forces in determining the solid-state structures. We have thus examined the physical properties of these materials by other solution phase methods as well as by computational methods. In solution these four compounds all face the same steric profile about the P=C unit, and thus should encounter the same barrier for rotation about P–Ar and C(H)–Ar bonds.

Table 1. Crystallographic data for compounds **8**, **9**, **10**, and **12**.

Compound	**8**	**9**	**10**	**12**
Empirical formula	$C_{31}H_{30}NO_2P$	$C_{32}H_{30}NP$	$C_{33}H_{32}NOP$	$C_{32}H_{33}OP$
Formula weight [g/mol]	479.53	459.54	489.57	464.55
Temperature [K]	100(2)	273(2)	100(2)	100(2)
Wavelength [Å]	0.71073	0.71073	0.71073	0.71073
Crystal system	monoclinic	monoclinic	triclinic	monoclinic
Space group	$P2_1/c$	$P2_1/n$	$P\bar{1}$	$P2_1/c$
Unit cell dimensions				
a [Å]	23.2380(6)	8.8864(3)	12.408(4)	13.1255(16)
b [Å]	8.2716(2)	13.3717(5)	13.525(5)	8.3261(10)
c [Å]	13.8440(4)	21.7122(7)	19.559(9)	24.814(3)
α [°]	90	90	100.417(7)	90
β [°]	101.539(2)	93.848(2)	101.084(7)	101.8120(10)
γ [°]	90	90	114.306(4)	90
Volume [Å^3]	2607.25(12)	2574.16(15)	2808.8(18)	2654.3(6)
Z	4	4	4	4
Calcd. density [Mg/m^3]	1.222	1.186	1.158	1.162
Absorption-coeff [mm]$^{-1}$	0.133	0.127	0.123	0.125
F(000)	1016	976	1040	992
Crystal size [mm]	$0.26 \times 0.12 \times 0.07$	$0.32 \times 0.22 \times 0.22$	$0.18 \times 0.11 \times 0.10$	$0.35 \times 0.28 \times 0.20$
θ range	0.89–26.00°	1.79–23.14°	1.11–26.00°	1.59–27.50°
Limiting indices	$-28 \le h \le 28$	$-9 \le h \le 9$	$-15 \le h \le 15$	$-17 \le h \le 17$
	$-10 \le k \le 9$	$-14 \le k \le 14$	$-16 \le k \le 16$	$-10 \le k \le 10$
	$-15 \le l \le 17$	$-23 \le l \le 23$	$-24 \le l \le 24$	$-32 \le l \le 32$
Reflections collected	18803	31244	30129	30125
Reflections unique	5124	3637	11001	6043
$R_{(int)}$	0.0504	0.0543	0.1048	0.0252
Completeness to θ	26.00°, 99%	23.14°, 99.9%	26.00°, 99.6%	27.50°, 99.3%
Absorption correction	multiscan			
Max. / min. transmission	0.991 / 0.981	0.9726 / 0.9605	0.9878 / 0.9783	0.9754 / 0.9575
Refinement method	full-matrix least squares on F^2			
Data	5124	3637	11001	6043
Restraints	0	0	0	0
Parameters	322	313	663	362
Goodness-of-fit on F^2	1.049	1.093	1.093	1.025
Final R indices[$I > 2\sigma(I)$]	R_1 = 0.0504	R_1 = 0.0599	R_1 = 0.0634	R_1 = 0.0427
	wR_2 = 0.1234	wR_2 = 0.1317	wR_2 = 0.1048	wR_2 = 0.1136
R indices (all data)	R_1 = 0.0768	R_1 = 0.0766	R_1 = 0.1625	R_1 = 0.0491
	wR_2 = 0.1449	wR_2 = 0.1442	wR_2 = 0.1434	wR_2 = 0.1196

Table 2. Selected structural data for **8**, **9**, **10**, and **12**.

	P=C bond length [Å]	C–P–C bond angles [°]	α_1[a]	α_2[b]
8	1.657(2)	105.5(1)	39.3°	19.3°
9	1.604(4)	105.9 (2)	46.5°	9.8°
10[c]	1.655(4)	104.0(2)	66.3°	11.4°
	1.649(4)	103.9 (2)	81.2°	3.6°
12	1.672(1)	103.3(7)	50.8°	18.3°

[a] Angle between the P-phenyl ring and C–P=C–C plane. [b] Angle between C(H)-phenyl ring and C–P=C–C plane. [c] Data for 2 unique molecules in the unit cell.

Theoretical Studies

The interplay between structural distortions and the effect of various groups on the structural properties of *meta*-terphenyl phosphaalkenes was examined in more detail through combined computational DFT (B3LYP/6-31+G**) and TDDFT (TD-B3LYP/6-31+G**) studies for the ground state and excited-state electronic structures, respectively. Full structural optimizations with DFT and calculations of the lowest singlet excitation (S_1 and S_2) electronic structures with TDDFT for several model compounds of

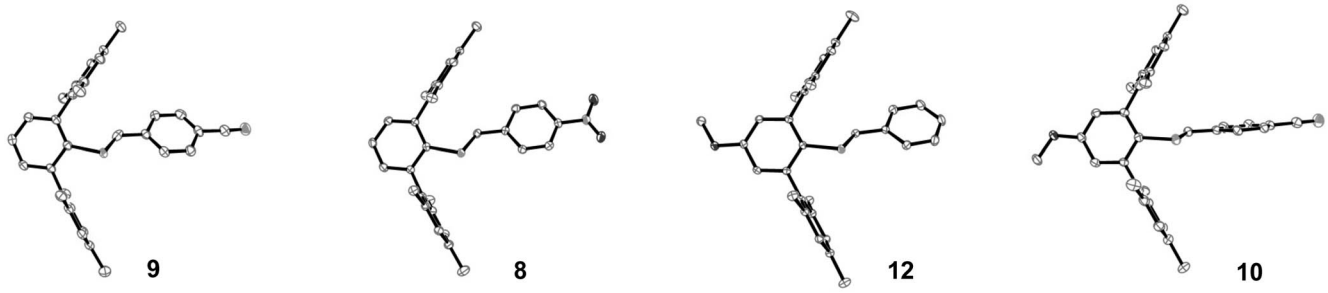

Figure 4. Structural comparisons between phosphaalkenes **8**, **9**, **10**, and **12**.

Table 3. Minimized structures of model phosphaalkenes by DFT (B3LYP/6-31+G**) and TDDFT (TD-B3LYP/6-31+G**).

	X	X′	$S_1(\pi–\pi^*)$ [eV]	$S_1(\pi–\pi^*)$ [nm] [a]	f[$S_1(\pi–\pi^*)$]	P=C bond lengths [Å]	C–P=C bond angles [°]	α_1 [°][b]	α_2 [°][c]
7′	H	H	3.42	363 (331)	0.61	1.695	103.1	32.9	6.1
8′	H	NO_2	3.06	406 (377)	0.73	1.695	103.6	30.5	8.2
9′	H	CN	3.26	380 (352)	0.77	1.695	103.4	31.5	8.1
10′	MeO	CN	3.02	410 (351)	0.73	1.695	104.0	28.5	9.7
11′	MeO	NO_2	2.80	443 (376)	0.70	1.695	104.2	27.2	9.9
12′	MeO	H	3.22	385 (332)	0.59	1.695	103.5	31.5	10.2

[a] Number in parenthesis is experimental value for related compound. [b] Angle between the P-phenyl ring and C–P=C–C plane. [c] Angle between C(H)-phenyl ring and C–P=C–C plane.

the form (*E*)-4-X-C_6H_4P=C(H)C_6H_4-4-X′ (**7′**–**12′**) were thus undertaken (Table 3, further data available in the Supporting Information).

For the ground-state structures, the P=C bond lengths were consistent at a distance of 1.695 Å (Table 3). Since the sterically encumbering mesityl groups were removed for computational simplicity, the α_1 angles determined by DFT were somewhat smaller than for the experimentally observed compounds, and ranged from 27.2–32.9°. The complimentary interplanar angles, α_2, are in much better agreement. The larger interplanar angles α_1 relative to α_2 derives from the more acute C–P–C bond angles and the larger size of phosphorus.

The S_1 transition was assigned as a $[\pi–\pi^*]_{PC}$ excitation and is the most intense band in the UV/Vis spectrum. A second transition, S_2, is predicted be a very weak $[n–\pi^*]_{PC}$ excitation. The computed $S_1(\pi–\pi^*)$ wavelengths reflect the trend observed experimentally. For example, redshifts of 21 nm and 46 nm on going from X′ = H (**7**) to X′ = CN (**9**) and NO_2 (**8**), respectively. This compares very well to the computed redshifts of 17 and 43 nm for the analogous model compounds X′ = H (**7′**) to X′ = CN (**9′**) and NO_2 (**8′**), respectively. Likewise, redshifts of 19 and 44 nm in 4-MeO-2,6-$Mes_2C_6H_2$P=C(H)C_6H_4-4-X′, on going from X′ = H (**12**) to X′ = CN (**10**) and NO_2 (**11**), are reproduced nicely in the computed redshifts of 25 and 58 nm on going from X′ = H (**12′**) to X′ = CN (**10′**) and NO_2 (**11′**), for the analogous model compounds.

Interestingly, the calculations also predict that substitution of electron-donating groups at the other end of the molecule should have a significant impact on the UV/Vis spectrum. For the minimum energy geometries, a redshift of 22 nm is calculated for the substitution of X = H (**7′**) to MeO (**12′**), while the analogous pair of experimental compounds **7** and **12** show a λ_{max} difference of only 1 nm.

The most likely origin of this difference is that the α_1 angle is smaller for the computed structures relative to the experimental values. Therefore constrained geometry optimizations and excitational energy calculations were performed on the model phosphaalkenes C_6H_5P=C(H)C_6H_5 (**7′**) and 4-MeO-C_6H_4P=C(H)C_6H_5 (**12′**) across a range of α_1 (Figure 5).

Compound **12′** exhibits complex behavior relative to the parent complex **7′**. First, the S_1 excitation of **12′** is redshifted relative to **7′**, while the S_2 energies are the same. Further, S_1 energies of **12′** are relatively invariant to α_1. Unsubstituted **7′** shows a significant blueshift upon increasing α_1. The S_2 excitation in both cases redshifts upon increasing α_1.

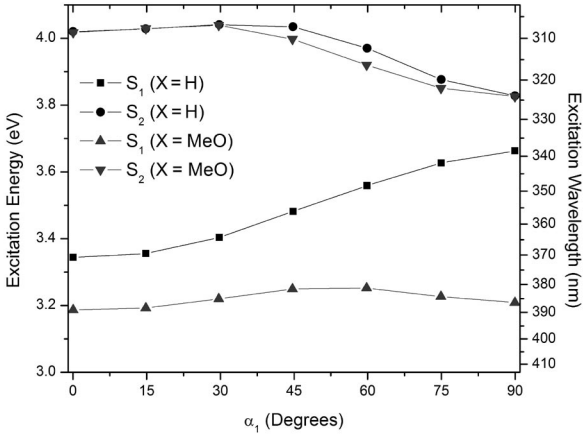

Figure 5. S_1 and S_2 excitation energies (left scale) and wavelengths (right scale) vs. α_1 angle for **7′** and **12′**.

At face value, these results do not seem to match the experimental data. However it is important to recall that the character of S_1 and S_2 are also a function of the α_1 coordinate via an avoided crossing. At α_1 = 0°, S_1 and S_2 states are easily assigned as S(π–π*) and S(n–π*), respectively. At α_1 = 90°, the S_1 and S_2 are switched to S(n–π*) and S(π–π*) respectively. In between 0° and 90°, the transitions are progressively mixed (n–π*) and (π–π*) in nature. Such mixing leads to the complex trends shown in Figure 5. Analogous features can be observed in the Kohn–Sham molecular orbitals (see Supporting Information).

With the dynamic nature of the character of S_1 and S_2 in mind, an estimate of the α_1 value for the experimental systems can be made based on the calculated excitation energies and oscillator strengths. Experimentally, the unsubstituted (**7**) and methoxy-substituted (**12**) compounds exhibit λ_{max} at 331 nm and 332 nm, respectively, and weak shoulders slightly redshifted from λ_{max}. The dominant band is assigned to the S(π–π*) excitation and the weaker shoulders to S(n–π*). The ordering implies a larger α_1 for the experimental compounds compared to the calculated minimum energy structures of the model compounds. From the ratio of the calculated oscillator strengths of the S_1 and S_2 excitations, the S_2 becomes the dominant band when 70° < α_1 < 90° for **7′** and S_2 is the dominant band when 60° <

$a_1 < 90°$ for **12′** respectively. In this regime, S_2 character is dominated by S(π–π*), the calculated S_2 excitation energies are practically the same for **7′** and **12′** which seems to be consistent with the experimentally observed spectra.

Electrochemical Studies

While UV/Vis spectroscopy can provide information about differences between ground-state and excited-state energies, electrochemical methods can provide insights to energies for oxidation and reduction of molecules, and thus yield experimental information on HOMO and LUMO energies. Phosphorus–carbon double bonds are weaker than carbon–carbon double bonds, and thus the π and π* orbitals of the P=C unit lie at higher and lower energies, respectively, than for corresponding C=C containing materials. This fact is evidenced by the UV/Vis data discussed above. The drop in energy of the π* orbitals of phosphaalkenes makes them susceptible to reduction by either chemical or electrochemical means. The radical anions that are generated can display varying degrees of stability, and cyclic voltammetry experiments can show reversible electrochemistry for these reduction/oxidation waves. The electrochemical redox properties of phosphaalkenes were first reported by Schoeller for a phosphaalkene that showed an irreversible redox processes in the cyclic voltammogram.[29] Later investigations revealed that redox processes can be quasi reversible, depending on the nature of groups bonded to the phosphorus–carbon double bond.[30–32]

Compounds **7**, **9**, **10**, and **12** were selected for study by cyclic voltammetry. The scans are displayed in Figures 6, 7, 8, and 9, and the specific potential data is summarized in Table 4. Each experiment was conducted in THF with [nBu$_4$N][BF$_4$] as the electrolyte, and in the presence of ferrocene as a reference (the left-most wave in each scan). Potentials are thus corrected for the known potential of ferrocene vs. SCE. As anticipated, each phosphaalkene displayed an apparently reversible reduction process. The CN substituent

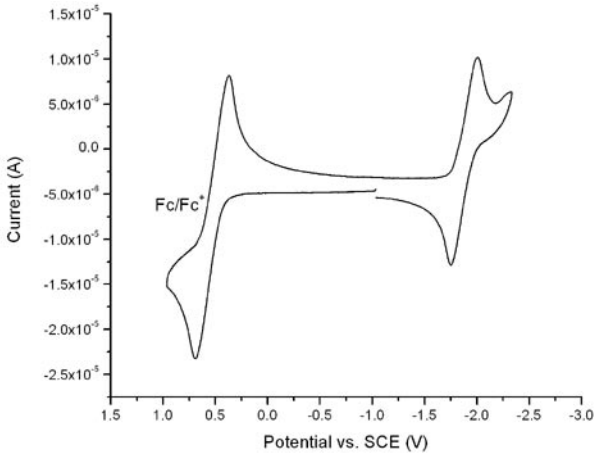

Figure 6. Cyclic voltammogram of **7**, 0.001M/0.001 M ferrocene in 0.1 M [nBu$_4$N][BF$_4$] in THF with 0.1 V/s scan rate.

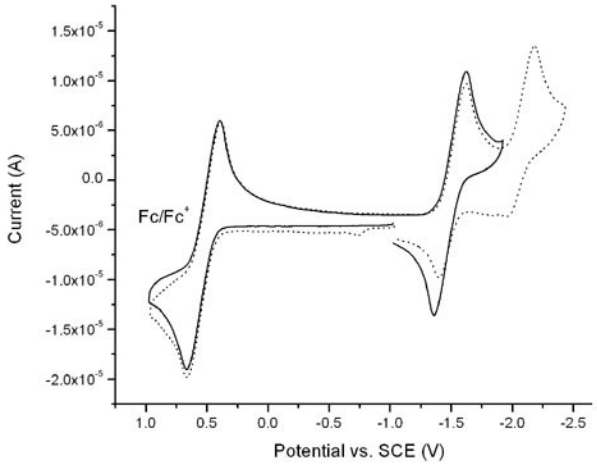

Figure 7. Cyclic voltammogram of **9**, 0.001M/0.001 M ferrocene in 0.1 M [nBu$_4$N][BF$_4$] in THF with 0.1 V/s scan rate, an overlay of the second redox potential shown in dotted lines.

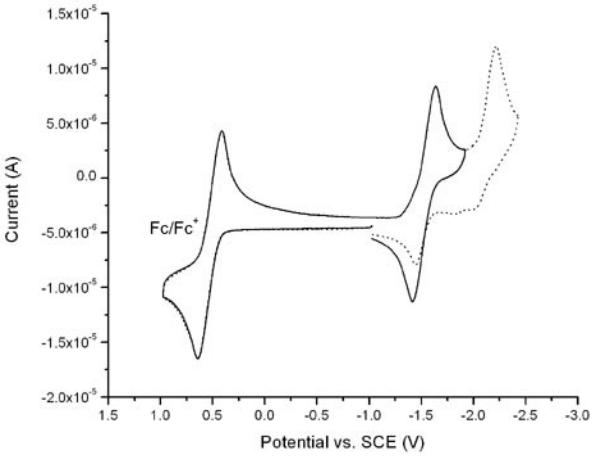

Figure 8. Cyclic voltammogram of **10**, 0.001M/0.001 M ferrocene in 0.1 M [nBu$_4$N][BF$_4$] in THF with 0.1 V/s scan rate, an overlay of the second redox potential shown in dotted lines.

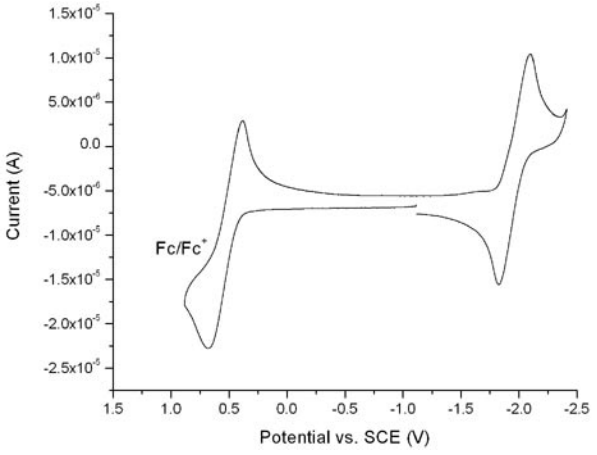

Figure 9. Cyclic voltammogram of **12**, 0.001M/0.001 M ferrocene in 0.1 M [nBu$_4$N][BF$_4$] in THF with 0.1 V/s scan rate.

in **9** and **10** shifts this potential positive by about 400 mV from that seen for **7**. The addition of the MeO group on going from **7** to **12**, and from **9** to **10**, however, makes the reduction more difficult by much smaller amounts (80 and 40 mV, respectively). These results can be ascribed to the same geometrical factors already discussed above. Similarly, the diphosphenes investigated bearing the diarylamino substituted terphenyl ligands did not display significantly shifted reductions in their cyclic voltammograms.[19,20]

Table 4. Electrochemcial data for phosphaalkenes (in V vs. SCE).

	E_c	E_a	$E_{1/2}$	E'_c
7	–2.02	–1.74	–1.88	–
9	–1.64	–1.34	–1.49	–2.20
10	–1.66	–1.40	–1.53	–2.23
12	–2.10	–1.83	–1.96	–

Cyano substituted species **9** and **10** both show evidence of a second accessible reductive process around –2.1 V vs. SCE. This reduction is definitely not reversible on the timescale of the experiment, and is near the reduction potential for stilbene.[33] One possible sequence for the two-step reduction of **9** and **10** is presented in Scheme 6.

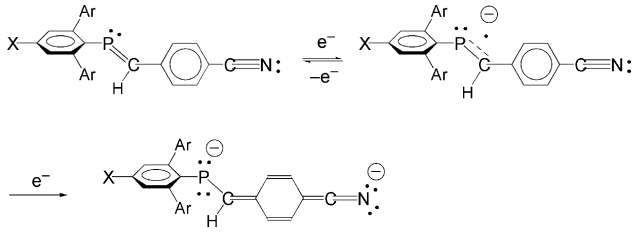

Scheme 6.

The results of these electrochemical investigations reinforce the importance of the X′ groups over the X groups in modulating the properties of this class of phosphaalkenes.

Nonlinear Optical Studies

Because alkenes that are polarized by the presence of donor and acceptor groups are often studied for nonlinear optical properties, phosphaalkenes **7**, **10**, and **11** were briefly examined by HRS (hyper Rayleigh scattering) experiments in attempts to measure the "β" component.[16] The HRS method is an alternative technique to the commonly used EFISH (electric field induced second harmonic generation) technique.[34,35] This approach has the advantage of measuring the "β" component without exposure to the external field and is much simpler than EFISH. The main disadvantage of HRS is that the scattered signals will be weak in intensity. Samples of phosphaalkenes in chloroform (ca. 500 μM) in quartz cuvettes excited with 1064 nm wavelength, however, showed no frequency doubling. Compounds **10** and **11** may not be polarized sufficiently by the donor and acceptor groups, or be reactive in other ways to the high power laser irradiation.

Conclusions

meta-Terphenyl phosphaalkenes with various substituents were synthesized and fully characterized. Four of these new compounds were examined by single-crystal X-ray diffraction methods, and the solid-state structures were determined. As the polarization across the P=C unit increased by the presence of electron-donating and electron-withdrawing substituents, reaching a maximum with compound **12**, the overall geometry of the phosphaalkenes was less suited for π-conjugation of the directly attached aryl rings to the central P=C unit. Analysis of the accumulated physical data, in particular of the UV/Vis absorption spectra, show that *para*-substituents on the less hindered phenyl rings about the P=C group resulted in more pronounced effects on the physical properties of the set of phosphaalkenes. These results were further corroborated by DFT and TDDFT calculations. Overall, the additive impact of the two *para*-substituents X and X′ are not as effective as found in related alkenes; hence, the use of stilbene-like phosphaalkenes in applications demanding a high degree of polarization, such as NLO materials, seems limited.

Experimental Section

General Procedures: All manipulations and syntheses were performed in an MBraun Labmaster nitrogen glove box or using standard vacuum line techniques under N_2. UV/Vis absorption data were recorded with a Cary 500 UV/Vis spectrometer. Chloroform was degassed with N_2. Tetrahydrofuran, diethyl ether and hexanes were dried by distilling over metallic sodium and benzophenone. Acetonitrile was dried with calcium hydride and distilled under nitrogen. Melting points were recorded using a Mel-Temp instrument. NMR spectra were recorded with a 400 MHz Varian-Inova Instrument using $CDCl_3$ as solvent. $^{31}P\{^1H\}$ NMR spectra are referenced to 85% H_3PO_4 as an external standard. The compounds 2,6-$Mes_2C_6H_3I$,[36] 2,6-$Mes_2C_6H_2PCl_2$,[37] and 2,6-$Mes_2C_6H_3P$=C(H)C_6H_5 (**7**),[23] 2,6-$Mes_2C_6H_3P$=C(H)C_6H_4-4-NO_2 (**8**)[23] were prepared by reported procedures. For several compounds, submission of samples for elemental analytical data did not return satisfactory detail, despite the fact that such materials displayed ^1H and ^{31}PNMR spectra that suggested >95% purity. This fact, especially for $ArPCl_2$, is likely due to sensitivity to air and water.

Computational Studies: Theoretical calculations employed the Gaussian03[38] software package and performed in parallel on Intel Pentium 4 Xeon EM64T quad-core processors. Time-dependent density-functional theory (TDDFT) and Kohn–Sham-formalized density-functional theory (DFT) were employed to calculate the excitation energies and ground state structures, respectively, with the B3LYP hybrid functional and 6-31+G(d,p) basis set.[39–49] B3LYP has proven to be a versatile functional, suitable for low-energy excitations and perturbations calculated in this paper. The justification of the level of theory for molecules of this class has been discussed elsewhere.[50] First, a small set of donor and acceptor groups (X and X′ = MeO, Me, H, CN, and NO_2) were substituted onto two model systems [i.e., (*E*)-4-X-C_6H_4-P=C(H)-C_6H_5 and (*E*)-C_6H_5P=C(H)C_6H_4-4-X′]. These models were fully structurally optimized and their lowest energy singlet excitations were calculated. Frequency calculations were performed on the all minimum energy structures. No imaginary frequency found indicating that the final structures are true minima. The model core struc-

tures are sufficient to describe the excitations observed in the experimental absorption spectra, which are primarily P=C and ring-based transitions. In addition, constrained geometry optimizations were performed for two model aryl-phosphaalkenes [(*E*)-4-X-$C_6H_4P{=}C(H)C_6H_5$, X = H, MeO] by scanning over a single ring twist dihedral coordinate denoted as α_1. Optimizations were performed on the ground state with a single constraint on α_1 at every 15° from α_1 = 0° to α_1 = 90°. The six lowest singlet excitation energies were calculated at each point.

Electrochemical Experiments: Cyclic voltammetry experiments were performed using a CH Instrument (CHI630C) workstation in a glove box under nitrogen. The supporting electrolyte, tetrabutylammonium tetrafluoroborate (Fluka), was recrystallized four times using 1:3 concentrated solutions of ethyl acetate and diethyl ether. The electrolyte was dried thoroughly under vacuum at 100–120 °C and stored in the drybox. Ferrocene was purified by sublimation. A glassy carbon working electrode was polished with 0.05 micron alumina and thoroughly cleaned and dried before use. A silver wire was utilized as a quasi-reference electrode and a platinum wire as the counter electrode. All scans were performed at a scan rate of 0.1 V/s with a potential window of approximately –3 to +1.5 V vs. saturated calomel electrode (SCE).

4-Br-2,6-$Mes_2C_6H_2Br$ (1):[20] To a 500 mL flask charged with 9.20 g (378 mmol) of activated Mg turnings was added slowly, through a double-ended metal cannula needle, 47.4 g (239 mmol) of bromomesitylene (Sigma–Aldrich) in 200 mL of THF. The exothermic reaction was moderated using a chilled water bath and then stirred for 6 h at room temperature. The solution was separated from unreacted Mg by transfer to a new flask and brought to reflux. To this solution was added through a cannula needle 31.4 g (71.3 mmol) of 2,4,6-tribromoiodobenzene in 150 mL of THF, and the solution was refluxed for 15 h. The solution was cooled by an ice bath, and 26.2 g (164 mmol) bromine was slowly added. The solution was stirred at room temperature for 2 h and then was quenched with 5% aqueous Na_2SO_3 (2 × 150 mL). The mixture was extracted with diethyl ether (2 × 200 mL) and the organic layers were combined and dried with Na_2SO_4. Removal of the volatiles by rotary evaporation gave a dark brown slurry, to which *n*-pentane was added in small amounts (15 mL) and left overnight at –6 °C. A pale brown solid was collected by filtration, and washed with 10 mL of *n*-pentane, and then dried to provide 20.2 g (30.0%) of **1** as a pale brown solid; m.p. 205–208 °C. ^{1}H NMR ($CDCl_3$): δ = 7.28 (s, 2 H), 6.95 (s, 4 H), 2.34 (s, 6 H), 2.01 (s, 12 H) ppm. $^{13}C\{^1H\}$ NMR ($CDCl_3$): δ = 144.9, 137.8, 137.6, 135.7, 132.2, 128.4, 125.5, 121.7, 21.5, 20.4 ppm. $C_{24}H_{24}Br_2$ (472.26): calcd. C 61.04, H 5.12; found C 59.84, H 4.82.

4-I-2,6-$Mes_2C_6H_2Br$ (2): To a solution of 2.16 g (4.58 mmol) of **1** in 100 mL of THF at –78 °C was slowly added 2.10 mL (5.57 mmol) of *n*BuLi (2.5M hexanes, Aldrich). The solution was stirred for 2 h and then 2.30 g (9.16 mmol) of solid iodine was added. The mixture was warmed to room temperature, and the excess iodine was quenched with 5% aqueous solution of Na_2SO_3. The mixture was extracted with diethyl ether (2 × 100 mL), and the organic layers combined and washed with water and brine (saturated) respectively, and dried with anhydrous Na_2SO_4. Removal of volatiles under vacuum yielded **2** as a colorless solid (1.62 g, 68.0%); m.p. 216–218 °C. ^{1}H NMR ($CDCl_3$): δ = 7.46 (s, 2 H), 6.94 (s, 4 H), 2.33 (s, 6 H), 2.01 (s, 12 H) ppm. $^{13}C\{^1H\}$ NMR ($CDCl_3$): δ = 144.9, 137.9, 137.6, 137.2, 135.5, 128.2, 126.5, 92.9, 21.2, 20.2 ppm.

4-(CH_3CONH)-2,6-$Mes_2C_6H_2Br$ (3): To a solution of 5.00 g (9.63 mmol) of **2** in 100 mL of THF in a 250 mL round-bottomed flask were added 0.37 g (1.9 mmol) of cuprous iodide, 3.80 mL (3.85 mmol) of *trans*-1,2-diaminocyclohexane, 0.68 g (12 mmol) of acetamide, and 2.66 g (19.3 mmol) of K_2CO_3. The reaction mixture was refluxed for 48 h with monitoring by NMR spectroscopic analysis of aliquots of the mixture to ascertain completion of reaction. The mixture was cooled to room temperature and extracted with diethyl ether (2 × 150 mL). The organic layers were combined and washed with water (2 × 100 mL) and with saturated brine solution (2 × 100 mL). The organic layer was separated and dried with anhydrous Na_2SO_4. Removal of the volatiles under vacuum yielded a brown colored material, which on purification by column chromatography using neutral silica gel with hexanes/ethyl acetate (60:40) as eluent gave 2.12 g of **3** (49.0%) as a pale brown powder; m.p. 276–278 °C. ^{1}H NMR ($CDCl_3$): δ = 7.32 (s, 2 H), 7.10 (s, 1 H), 6.94 (s, 4 H), 2.33 (s, 6 H), 2.17 (s, 3 H), 2.01 (s, 12 H) ppm. $^{13}C\{^1H\}$ NMR ($CDCl_3$): δ = 168.2, 143.3, 138.2, 137.7, 137.2, 135.5, 128.1, 120.5, 120.1, 24.7, 21.2, 20.2 ppm. $C_{26}H_{28}BrNO$ (450.42): calcd. C 69.33, H 6.27, N 3.11; found C 69.03, H 6.25, N 2.90.

4-(H_2N)-2,6-$Mes_2C_6H_2Br$ (4): To a solution of 0.50 g (1.1 mmol) of **3** in 50 mL of THF was added 50 mL of 1 N HCl solution. The mixture was refluxed for 20 h, after which time ^{1}H NMR analysis of a reaction aliquot indicated the disappearance of the amide protons of **3**. The reaction mixture was cooled to room temperature, and 2 N NaOH was added slowly until the reaction mixture became slightly basic. The product was then extracted using $CHCl_3$ (2 × 100 mL). Removal of volatiles under vacuum gave 0.42 g (92%) of **4** as a pale brown-colored solid; m.p. 214–216 °C. ^{1}H NMR ($CDCl_3$): δ = 6.93 (s, 4 H), 6.47 (s, 2 H), 3.70 (s, 2 H), 2.32 (s, 6 H), 2.04 (s, 12 H) ppm. $^{13}C\{^1H\}$ NMR ($CDCl_3$): δ = 145.9, 143.3, 138.8, 136.9, 135.6, 127.9, 115.9, 114.1, 21.2, 20.1 ppm. $C_{24}H_{26}BrN$ (408.38): calcd. C 70.59, H 6.42, N 3.43; found C 69.22, H 5.89, N 3.19.

4-[($CH_3)_2N$]-2,6-$Mes_2C_6H_2Br$ (5a): In a 100 mL round-bottomed flask, 5.00 g (12.2 mmol) of **4** and 12.2 g (320 mmol) of $NaBH_4$ was dissolved in 30 mL of THF. This slurry was added to a 100 mL flask containing 30.0 mL (380 mmol) of HCHO (37% wt./wt., Fischer), 10 mL H_2SO_4 and 10 mL of THF at 0 °C over a period of 10 min. The reaction mixture was allowed to reach room temperature and was stirred for 5 h, at which time it was chilled in an ice bath and water was added to quench the reaction. The reaction mixture was extracted with (2 × 100 mL) $CHCl_3$, and the organic phase separated. The volatiles were removed under vacuum, and the resulting material was further purified by column chromatography using neutral silica gel with (80:20) hexanes/ethyl acetate as eluent. Compound **5a** was thus isolated as a pale brown solid (4.50 g, 85.0%); m.p. 173–175 °C ^{1}H NMR ($CDCl_3$): δ = 6.95 (s, 4 H), 6.47 (s, 2 H), 2.91 (s, 6 H), 2.34 (s, 6 H), 2.06 (s, 12 H) ppm. $^{13}C\{^1H\}$ NMR ($CDCl_3$): δ = 149.9, 142.7, 139.5, 136.9, 135.8, 127.9, 113.0, 111.9, 40.6, 21.2, 20.2 ppm. $C_{26}H_{30}BrN$ (436.43): calcd. C 71.55, H 6.93, N 3.21; found C 71.49, H 7.02, N 3.17.

4-CH_3O-2,6-$Mes_2C_6H_2Br$ (5b): A mixture of 5.00 g (9.60 mmol) of **2**, 0.48 g (2.4 mmol) of *ortho*-phenanthroline, 0.18 g (0.96 mmol) of cuprous iodide, and 7.60 g (48.2 mmol) of KF/Al_2O_3 (37.0%)[51] was prepared in 100 mL of THF. 250 mL of methanol was added, and the mixture was refluxed for 48 h. The mixture was cooled to room temperature and extracted using dichloromethane (2 × 150 mL). The organic layers were combined and washed with water (2 × 100 mL) and with saturated brine (2 × 100 mL). The organic layer was separated and dried with anhydrous Na_2SO_4. The volatiles were removed under vacuum to give a solid material that was purified by column chromatography using neutral silica gel

with hexanes/dichloromethane (95:5) as the eluent. Compound **5b** was thus isolated as a colorless powder (3.12 g, 70.0%); m.p. 117–120 °C. ^{1}H NMR ($CDCl_3$): δ = 6.95 (s, 4 H), 6.69 (s, 2 H), 3.77 (s, 3 H), 2.34 (s, 6 H), 2.03 (s, 12 H) ppm. $^{13}C\{^1H\}$ NMR ($CDCl_3$): δ = 151.3, 143.7, 138.8, 137.4, 135.8, 128.4, 116.8, 114.9, 55.7, 21.5, 20.4 ppm. $C_{25}H_{27}BrO$ (423.39): calcd. C 70.92, H 6.43; found C 70.95, H 6.49.

4-[$(CH_3)_2N$]-2,6-$Mes_2C_6H_2PCl_2$ (6a): To a solution of 0.50 g (1.2 mmol) of **5a** in 40 mL of THF at –78 °C was slowly added 0.70 mL (1.7 mmol) of *n*BuLi (2.5 M in hexanes, Sigma–Aldrich). The mixture was stirred at –78 °C for 2.5 h. Then, 0.30 mL (3.4 mmol) of PCl_3 was added at once, and the solution was allowed to reach room temperature. The solvent and excess PCl_3 were removed under vacuum from the now yellowish-orange colored solution. The resulting material was then dissolved in hexanes and filtered through a bed of Celite. Removal of hexanes under vacuum gave 0.16 g (30%) of **6a** as a colorless solid; m.p. 52–54 °C. ^{1}H NMR ($CDCl_3$): δ = 6.93 (s, 4 H), 6.36 (s, 1 H), 6.35 (s, 1 H), 3.00 (s, 6 H), 2.34 (s, 6 H), 2.10 (s, 12 H) ppm. $^{31}P\{^1H\}$ NMR ($CDCl_3$): δ = 163.7 ppm. $^{13}C\{^1H\}$ NMR ($CDCl_3$): δ = 152.9, 148.4 (d, J_{PC} = 31 Hz), 137.6, 137.3, 136.9, 128.0, 113.1, 40.2, 21.5, 21.4 ppm.

4-CH_3O-2,6-$Mes_2C_6H_2PCl_2$ (6b): To a solution of 0.50 g (1.2 mmol) of **5b** in 50 mL of THF at –78 °C was slowly added 0.70 mL (1.5 mmol) of *n*BuLi (2.5 M, hexanes, Sigma–Aldrich). The reaction mixture was stirred at –78 °C for 2.5 h. Then 0.50 mL (5.9 mmol) of PCl_3 (Sigma–Aldrich) was added all at once, and the mixture was warmed to room temperature. The solvent and excess PCl_3 was removed in vacuo from the now orange colored solution, yielding a pale orange-colored sticky solid. The material was dissolved in hexanes and filtered through Celite. Evaporation of the hexanes gave a sticky material. The procedure was repeated two more times. Dissolution of the material once again in hexanes, followed by addition of a few drops of acetonitrile, resulted in the precipitation of **6b** as a white solid. Compound **6b** was collected by filtering through a glass frit and dried under vacuum (0.31 g, 50%); m.p. 122–124 °C. ^{1}H NMR ($CDCl_3$): δ = 6.92 (s, 4 H), 6.64 (s, 1 H), 6.63 (s, 1 H), 3.82 (s, 3 H), 2.34 (s, 6 H), 2.06 (s, 12 H) ppm. $^{31}P\{^1H\}$ NMR ($CDCl_3$): δ = 160.7 ppm. $^{13}C\{^1H\}$ NMR ($CDCl_3$): δ = 163.0, 149.2 (d, J_{CP} = 50.2 Hz), 137.9, 136.7 (d, J_{CP} = 2.8 Hz), 136.3 (d, J_{CP} = 7.6 Hz), 128.2, 126.0 (d, J_{CP} = 70.1 Hz), 116.1 (d, J_{CP} = 2.1 Hz), 55.7, 21.5, 21.4 ppm. $C_{25}H_{27}Cl_2OP$ (445.37): calcd. C 67.42, H 6.11; found C 68.19, H 6.59.

(*E*)-4-(4-Nitrostyryl)benzaldehyde:[52] In a 100 mL flask, 0.57 g (3.1 mmol) of 4-bromobenzaldehyde (Sigma–Aldrich), 0.46 g (3.1 mmol) 4-nitrostyrene, 0.020 g (0.096 mmol) of $Pd(OAc)_2$, 0.27 g (0.64 mmol) of tetraphenylphosphonium bromide and 1.31 g (16.0 mmol) of sodium acetate was added to 20 mL of anhydrous DMF. The solution refluxed for 24 h. The mixture was allowed to cool to room temperature and quenched by the addition of water (20 mL). The resulting mixture filtered under vacuum yielding a yellow solid. This solid was purified by column chromatography with neutral silica and ethyl acetate/hexanes (35:65) as eluent to yield 0.41 g (53%) of (*E*)-4-(4-nitrostyryl)benzaldehyde as a yellow solid; m.p. 63–65 °C. ^{1}H NMR ($CDCl_3$): δ = 10.02 (s, 1 H), 8.25 (d, J_{HH} = 9.2 Hz, 2 H), 7.91 (d, J_{HH} = 8.8 Hz, 2 H), 7.69 (t, J_{HH} = 8.8 Hz, 4 H), 7.29 (s, 2 H) ppm. $^{13}C\{^1H\}$ NMR ($CDCl_3$): δ = 191.5, 147.3, 142.9, 142.1, 136.2, 131.8, 130.3, 129.6, 127.5, 127.4, 124.3 ppm.

(*E*)-2,6-$Mes_2C_6H_3P$=C(H)C_6H_4-4-NO_2 (8):[23] To a 50 mL round-bottomed flask were added 0.50 g (1.2 mmol) of 2,6-$Mes_2C_6H_3PCl_2$, 0.080 g (1.3 mmol) of Zn dust and 7.20 mL (7.20 mmol) of PMe_3 (1.00 M in toluene, Sigma–Aldrich), and the resulting mixture was stirred for 3 h. To this mixture was added 0.18 g (1.2 mmol) of 4-nitrobenzaldehyde, and it was stirred for another 2 h. The solvent was removed under vacuum, leaving a dark red colored solid. The solid was extracted into hexanes and filtered through Celite. Removal of the hexanes under vacuum left a yellow colored solid. The solid was dissolved in diethyl ether and recrystallized at –35 °C to afford 0.25 g (43%) of **8** as a pale yellow solid; m.p. 132–136 °C. ^{1}H NMR ($CDCl_3$): δ = 8.55 (d, J_{PH} = 24.8 Hz, 1 H), 7.95 (d, J_{HH} = 8.9 Hz), 7.50 (t, J_{HH} = 7.6 Hz, 1 H), 7.20 (d, J_{HH} = 8.9 Hz, 2 H), 7.13 (d, J_{HH} = 7.6 Hz, 2 H), 6.88 (s, 4 H), 2.26 (s, 6 H), 2.04 (s, 12 H) ppm. $^{31}P\{^1H\}$ NMR ($CDCl_3$): δ = 268.5 ppm. $^{13}C\{^1H\}$ NMR ($CDCl_3$): δ = 176.5 (d, J_{PC} = 36. 4 Hz), 147.0 (s), 146.3 (d, J_{PC} = 15.4 Hz), 144.9 (d, J_{PC} = 8.5 Hz), 138.0 (d, J_{PC} = 3.0 Hz), 137.5 (s), 135.8 (s), 130.3 (s), 129.2 (s), 128.9 (s), 128.5 (s), 126.2 (d, J_{PC} = 21.3 Hz), 124.0 (d, J_{PC} = 1.7 Hz), 21.3 (s), 21.1 (s) ppm. λ_{max} = 377 nm, logε = 4.21.

(*E*)-2,6-$Mes_2C_6H_3P$=C(H)C_6H_4-4-CN (9): To a 50 mL round-bottomed flask were added a stir bar, 0.40 g (0.90 mmol) of **4b**, and 0.06 g (0.9 mmol) of Zn dust. To this flask was added 5.40 mL (5.40 mmol) of PMe_3 (1.00 M in toluene), and the mixture was stirred for 3 h. A sample of 0.12 g (0.90 mmol) of 4-cyanobenzaldehyde was then added and the mixture was stirred for 2 h. The solvent was removed under vacuum and the product was extracted into hexanes, and filtered through Celite. Removal of hexanes under vacuum gave the product which was purified by recrystallizing from a concentrated solution of **9** in diethyl ether at –35 °C. Compound **9** was isolated as a pale yellow solid after drying; m.p. 98–100 °C, yield 0.44 g (67%). ^{1}H NMR ($CDCl_3$): δ = 8.55 (d, J_{PH} = 24.8 Hz, 1 H), 7.49 (t, J_{HH} = 7.6 Hz, 1 H), 7.36 (d, J_{HH} = 8.3 Hz, 2 H), 7.16 (d, J_{HH} = 8.3 Hz, 2 H), 7.13 (d, J_{HH} = 7.6 Hz, 2 H), 6.88 (s, 4 H), 2.27 (s, 6 H), 2.05 (s, 12 H) ppm. $^{13}C\{^1H\}$ NMR ($CDCl_3$): δ = 177.0 (d, J_{PC} = 35.8 Hz), 144.7 (d, J_{PC} = 8.2 Hz), 144.1 (d, J_{PC} = 15.3 Hz), 140.2 (s), 137.9 (d, J_{PC} = 3.1 Hz), 137.2 (s), 135.5 (s), 132.1 (d, J_{PC} = 2.2 Hz), 130.0 (s), 128.6 (s), 128.2 (s), 126.0 (d, J_{PC} = 21.4 Hz), 119.0 (d, J_{PC} = 2.6 Hz), 110.7 (d, J_{PC} = 7.4 Hz), 21.1 (s), 20.9 (s) ppm. $^{31}P\{^1H\}$ NMR ($CDCl_3$): δ = 263.5 ppm. λ_{max} = 352 nm, logε = 4.32.

(*E*)-4-(CH_3O)-2,6-$Mes_2C_6H_2P$=C(H)C_6H_4-4-CN (10): To a 50 mL round-bottomed flask were added a stir bar, 0.40 g (0.90 mmol) of **6b**, and 0.06 g (0.9 mmol) of Zn dust. To this mixture was added 5.40 mL (5.40 mmol) of PMe_3 (1.00 M in toluene), and the mixture was stirred for 3 h. A sample of 0.12 g (0.90 mmol) of 4-cyanobenzaldehyde was added, and the mixture was stirred for 2 h. The solvent was removed under vacuum, and the product was extracted into hexanes and filtered through Celite. This process was repeated. Removal of volatiles under vacuum provided 0.44 g (67%) of **10** as a yellow colored solid; m.p. 108–110 °C. ^{1}H NMR ($CDCl_3$): δ = 8.42 (d, J_{PH} = 24.4 Hz, 1 H), 7.35 (d, J_{HH} = 8.4 Hz, 1 H), 7.13 (d, J_{HH} = 8.4 Hz, 2 H), 6.88 (s, 4 H), 6.69 (s, 2 H), 3.82 (s, 3 H), 2.27 (s, 6 H), 2.07 (s, 12 H) ppm. $^{13}C\{^1H\}$ NMR ($CDCl_3$): δ = 176.3 (d, J_{PC} = 35.2 Hz), 160.6 (s), 146.1 (d, J_{PC} = 9.1 Hz), 137.6 (s), 136.9 (s), 135.6 (d, J_{PC} = 6.0 Hz), 135.4 (s), 135.1 (s), 131.6 (s), 127.8 (s), 125.5 (d, J_{PC} = 20.8 Hz), 118.7 (s), 113.9 (s), 110.1 (s), 54.9 (s), 20.7 (s), 20.4 (s) ppm. $^{31}P\{^1H\}$ NMR ($CDCl_3$): δ = 262.6 ppm. λ_{max} = 351 nm, logε = 4.28.

(*E*)-4-(CH_3O)-2,6-$Mes_2C_6H_2P$=C(H)C_6H_4-4-NO_2 (11): To a clean 50 mL round-bottomed flask were added a stir bar, 0.50 g (1.1 mmol) of **6b**, and 0.080 g (1.2 mmol) of Zn dust. To this flask was added 6.70 mL (6.70 mmol) of PMe_3 (1.00 M in toluene), and the mixture stirred for 3 h. A sample of 0.17 g (1.1 mmol) of 4-nitrobenzaldehyde was added and the mixture was stirred for 10 min. The reaction mixture was filtered through Celite and the

solvent was removed under vacuum, leaving a dark red residue. This solid was extracted with 15 mL of hexanes, and the solution was filtered through Celite. The volatiles were removed under vacuum to provide 0.33 g (56%) of **11** as a dark yellow solid. ^{1}H NMR ($CDCl_3$): δ = 8.43 (d, J_{PH} = 24.4 Hz, 1 H), 7.92 (d, J_{HH} = 8.4 Hz, 2 H), 7.18 (d, J_{HH} = 8.4 Hz, 2 H), 6.88 (s, 4 H), 3.83 (s, 3 H), 2.27 (s, 6 H), 2.07 (s, 12 H) ppm. ^{13}C{^{1}H} NMR ($CDCl_3$): δ = 176.2 (d, J_{PC} = 36.4 Hz), 161.3 (s), 146.7 (d, J_{PC} = 9.5 Hz), 137.6 (s), 136.7 (s), 135.8 (s), 128.4 (s), 128.2 (s), 126.1 (d, J_{PC} = 21.3 Hz), 124.0 (s), 114.6 (s), 113.8 (s), 113.2 (s), 55.6 (s), 21.3 (s), 21.1 (s) ppm. ^{31}P{^{1}H} NMR ($CDCl_3$): δ = 267.0 ppm; m.p. 86–91 °C. λ_{max} = 376 nm, logε = 4.08.

(*E*)-4-(CH_3O)-2,6-$Mes_2C_6H_2P$=C(H)C_6H_5 (12): To a clean 50 mL round-bottomed flask was added a stir bar, 0.25 g (0.56 mmol) of **6b**, and 0.04 g (0.6 mmol) of Zn dust. To this flask was added 3.40 mL (3.40 mmol) of PMe_3 (1.00 M in toluene), and the mixture stirred for 3 h. A sample of 0.060 mL (0.59 mmol) of benzaldehyde was added, and the reaction stirred for 2 h. The reaction mixture was filtered through a glass frit, and the volatiles were removed under vacuum. The solid was extracted into hexanes and filtered. The solvent was removed under vacuum, and the product was rinsed with acetonitrile. The solid was dried under vacuum to give 0.15 g (47%) of **12** as a pale yellow colored solid; m.p. 202–204 °C. ^{1}H NMR ($CDCl_3$): δ = 8.59 (d, J_{PH} = 25.2 Hz, 1 H), 7.09 (m, 5 H), 6.87 (s, 4 H), 6.67 (s, 2 H), 3.81 (s, 3 H), 2.26 (s, 6 H), 2.08 (s, 12 H) ppm. ^{13}C{^{1}H} NMR ($CDCl_3$): δ = 180.1 (d, J_{PC} = 35.2 Hz), 160.7 (s), 146.6 (d, J_{PC} = 8.9 Hz), 140.6 (d, J_{PC} = 14.7 Hz), 138.6 (d, J_{PC} = 2.9 Hz), 137.2 (s), 135.7 (s), 132.4 (s), 128.4 (d, J_{PC} = 2.2 Hz), 128.3 (s), 128.1 (d, J_{PC} = 6.9 Hz), 125.9 (d, J_{PC} = 21.1 Hz), 114.3 (s), 55.5 (s), 21.3 (s), 21.1 (s) ppm. ^{31}P{^{1}H} NMR ($CDCl_3$): δ = 240.7 ppm. λ_{max} = 332 nm, logε = 4.27.

(*E*)-4-[$(CH_3)_2N$]-2,6-$Mes_2C_6H_2P$=C(H)C_6H_5 (13): To a 25 mL round-bottomed flask were added a stir bar, 0.10 g (0.21 mmol) of **6a**, and 0.020 g (0.25 mmol) of Zn dust. To this flask was added 1.28 mL (1.28 mmol) of PMe_3 (1.00 M in toluene), and the resulting mixture was stirred for 3 h. A sample of 0.030 mL (0.25 mmol) of benzaldehyde was then added, and the mixture was stirred for 2 h. The solution was filtered, and the volatiles were removed under vacuum. The product was extracted into hexanes, and the solution was filtered. The solvent was removed under vacuum and the resulting product was then recrystallized from a concentrated solution of diethyl ether at –35 °C. Following drying under vacuum compound **13** was isolated as yellowish orange solid (0.050 g, 40%); m.p. 116–118 °C. ^{1}H NMR ($CDCl_3$): δ = 8.47 (d, J_{PH} = 24.8 Hz, 1 H), 7.08 (m, 5 H), 6.88 (s, 4 H), 6.45 (s, 2 H), 2.97 (s, 6 H), 2.28 (s, 6 H), 2.11 (s, 12 H) ppm. ^{31}P{^{1}H} NMR ($CDCl_3$): δ = 242.5 ppm.

(*E*)-2,6-$Mes_2C_6H_3P$=C(H)C_6H_4C(H)=C(H)-C_6H_4-4-NO_2 (14): To a 50 mL dry round-bottomed flask were added a stir bar, 0.20 g (0.48 mmol) of 2,6-$Mes_2C_6H_3PCl_2$, and 0.040 g (0.51 mmol) of Zn dust. To this flask was addded 2.90 mL (2.90 mmol) of PMe_3 (1.00 M in toluene), and the mixture was stirred for 2 h. A sampe of 0.13 g (0.51 mmol) of (*E*)-4-(4-nitrostyryl)benzaldehyde was added and the reaction stirred for 2 h. The solution was filtered through Celite, the volatiles were removed under vacuum. The remaining solid was extracted into diethyl ether and the solution was filtered through Celite. The solvent was removed under vacuum and the resulting solid re-dissolved into hexanes and filtered through Celite. The solvent was removed under vacuum and this material was washed with small amount of acetonitrile. The product was dried under vacuum to give 0.21 g (75%) of **14** as a pale brownish-orange solid; m.p. 220–222 °C. ^{1}H NMR ($CDCl_3$): δ = 8.62 (d, J_{PH} = 24.8 Hz, 1 H), 8.19 (d, J_{HH} = 9.0 Hz, 2 H), 7.58 (d, J_{HH} = 9.0 Hz, 2 H), 7.45 (t, J_{HH} = 7.6 Hz, 1 H), 7.29 (d, J_{HH} = 8.0 Hz, 2 H), 7.02–7.17 (m, 6 H), 6.88 (s, 4 H), 2.27 (s, 6 H), 2.07 (s, 12 H) ppm. ^{13}C{^{1}H} NMR ($CDCl_3$): δ = 178.9 (d, J_{PC} = 35.6 Hz), 146.9 (s), 145.0 (d, J_{PC} = 8.0 Hz), 144.0 (s), 141.1 (d, J_{PC} = 13.2 Hz), 138.5 (s), 137.2 (s), 136.1 (d, J_{PC} = 7.4 Hz), 135.8 (s), 132.9 (d, J_{PC} = 2.6 Hz), 129.8 (s), 128.7 (s), 128.4 (s), 127.2 (s), 127.0 (s), 126.5 (d, J_{PC} = 21.4 Hz), 126.3 (s), 124.4 (s), 100.3 (s), 21.3 (s), 21.2 (s) ppm. ^{31}P{^{1}H} NMR ($CDCl_3$): δ = 245.1. λ_{max} = 402 nm, logε = 4.65 ppm.

(*E*)-4-(CH_3O)-2,6-$Mes_2C_6H_2P$=C(H)C_6H_4C(H)=C(H)-C_6H_4-4-NO_2 (15): To a 50 mL round-bottomed flask were added a stir bar, 0.20 g (0.45 mmol) of **6b**, and 0.030 g (0.47 mmol) of Zn dust. To this flask was added 2.70 mL (2.70 mmol) of PMe_3 (1.00 M in toluene), and the mixture was stirred for 3 h. A sample of 0.12 g (0.47 mmol) of (*E*)-4-(4-nitrostyryl)benzaldehyde was added, and the reaction was stirred 2 h. The reaction mixture was filtered and the volatiles were removed under vacuum. The solid was extracted into hexanes and filtered through Celite. Removal of hexanes gave a solid that was further purified by washing with small amounts of acetonitrile. The product was dried under vacuum to afford 0.20 g (71%) of **15** as a brownish-orange colored solid; m.p. 205–209 °C. ^{1}H NMR ($CDCl_3$): δ = 8.53 (d, J_{PH} = 24.4 Hz, 1 H), 8.19 (d, J_{HH} = 8.8 Hz, 2 H), 7.58 (d, J_{HH} = 8.8 Hz, 2 H), 7.27 (d, J_{HH} = 8.4 Hz, 2 H), 7.00–7.15 (m, 4 H), 6.88 (s, 4 H), 6.68 (s, 2 H), 3.82 (s, 3 H), 2.27 (s, 6 H), 2.09 (s, 12 H) ppm. ^{13}C{^{1}H} NMR ($CDCl_3$): δ = 178.6 (d, J_{PC} = 35.6 Hz), 160.6 (s), 146.7 (s), 146.4 (s), 143.8 (s), 141.1 (s), 138.3 (s), 137.0 (s), 135.7 (d, J_{PC} = 6.5 Hz), 135.5 (s), 132.8 (s), 131.7 (s), 128.1 (s), 126.9 (s), 126.7 (s), 126.2 (d, J_{PC} = 21.1 Hz), 125.9 (s), 124.1 (s), 114.2 (s), 55.3 (s), 21.0 (s), 20.9 (s) ppm. ^{31}P{^{1}H} NMR ($CDCl_3$): δ = 245.7 ppm. λ_{max} = 409 nm, logε = 4.66.

CCDC-746288 (for **8**), -746289 (for **9**), -746290 (for **10**), -746291 (for **12**) contain the supplementary crystallographic data for this paper. These data can be obtained free of charge from The Cambridge Crystallographic Data Centre via www.ccdc.cam.ac.uk/data_request/cif.

Supporting Information (see also the footnote on the first page of this article): Computational results (24 pages).

Acknowledgments

We thank the US National Science Foundation (NSF) for support (CHE-0748982, CHE-0518510, and CHE-0541766). We thank Prof. Kenneth D. Singer and Yeheng Wu (Department of Physics, Case Western Reserve University) for screening compounds for possible NLO activity.

[1] K. B. Dillon, F. Mathey, J. F. Nixon, *Phosphorus: The Carbon Copy*, John Wiley & Sons, New York, **1998**.
[2] F. Mathey, *Angew. Chem. Int. Ed.* **2003**, *42*, 1578.
[3] R. Appel, F. Knoll, I. Ruppert, *Angew. Chem. Int. Ed. Engl.* **1981**, *20*, 731.
[4] R. Appel, *Pure Appl. Chem.* **1987**, *59*, 977.
[5] R. Appel, F. Knoll, *Adv. Inorg. Chem.* **1989**, *33*, 259.
[6] F. Mathey, *Acc. Chem. Res.* **1992**, *25*, 90.
[7] L. N. Markovskii, V. D. Romanenko, *Tetrahedron* **1989**, *45*, 6019.
[8] L. Weber, *Eur. J. Inorg. Chem.* **2000**, 2425.
[9] S. Shah, J. D. Protasiewicz, *Coord. Chem. Rev.* **2000**, *210/1*, 181.
[10] R. C. Smith, J. D. Protasiewicz, *Eur. J. Inorg. Chem.* **2004**, 998.
[11] R. C. Smith, X. Chen, J. D. Protasiewicz, *Inorg. Chem.* **2003**, *42*, 5468.

[12] R. C. Smith, J. D. Protasiewicz, *J. Am. Chem. Soc.* **2004**, *126*, 2268.
[13] V. A. Wright, B. O. Patrick, C. Schneider, D. P. Gates, *J. Am. Chem. Soc.* **2006**, *128*, 8836.
[14] D. P. Gates, *Top. Curr. Chem.* **2005**, *250*, 107.
[15] V. A. Wright, D. P. Gates, *Angew. Chem. Int. Ed.* **2002**, *41*, 2389.
[16] S. R. Marder, *Chem. Commun.* **2006**, 131.
[17] A. Termaten, M. van der Sluis, F. Bickelhaupt, *Eur. J. Org. Chem.* **2003**, 2049.
[18] S. Kawasaki, A. Nakamura, K. Toyota, M. Yoshifuji, *Bull. Chem. Soc. Jpn.* **2005**, *78*, 1110.
[19] K. Tsuji, S. Sasaki, M. Yoshifuji, *Tetrahedron Lett.* **1999**, *40*, 3203.
[20] S. Sasaki, H. Aoki, K. Sutoh, S. Hakiri, K. Tsuji, M. Yoshifuji, *Helv. Chim. Acta* **2002**, *85*, 3842.
[21] L. Weber, P. Bayer, S. Uthmann, T. Braun, H.-G. Stammler, B. Neumann, *Eur. J. Inorg. Chem.* **2006**, 137.
[22] R. C. Fischer, L. Pu, J. C. Fettinger, M. A. Brynda, P. P. Power, *J. Am. Chem. Soc.* **2006**, *128*, 11366.
[23] S. Shah, J. D. Protasiewicz, *Chem. Commun.* **1998**, 1585.
[24] V. B. Gudimetla, A. L. Rheingold, J. L. Payton, H.-L. Peng, M. C. Simpson, J. D. Protasiewicz, *Inorg. Chem.* **2006**, *45*, 4895.
[25] E. A. Schmittling, J. S. Sawyer, *Tetrahedron Lett.* **1991**, *32*, 7207.
[26] A. Klapars, X. Huang, S. L. Buchwald, *J. Am. Chem. Soc.* **2002**, *124*, 7421.
[27] K. Toyota, S. Kawasaki, M. Yoshifuji, *J. Org. Chem.* **2004**, *69*, 5065.
[28] J. D. Protasiewicz, M. P. Washington, V. B. Gudimetla, manuscript in preparation.
[29] W. W. Schoeller, J. Niemann, R. Thiele, W. Haug, *Chem. Ber.* **1991**, *124*, 417.
[30] A. A. Badri, A. Jouaiti, M. Geoffroy, *Magn. Reson. Chem.* **1999**, *37*, 735.
[31] A. Jouaiti, A. A. Badri, M. Geoffroy, G. Bernardinelli, *J. Organomet. Chem.* **1997**, *529*, 143.
[32] M. Geoffroy, A. Jouaiti, G. Terron, M. Cattani-Lorente, Y. Ellinger, *J. Phys. Chem.* **1992**, *96*, 8241.
[33] H. Ndayikengurukiye, S. Jacobs, W. Tachelet, J. Van Der Looy, A. Pollaris, H. J. Geise, M. Claeys, J. M. Kauffmann, S. Janietz, *Tetrahedron* **1997**, *53*, 13811.
[34] K. Clays, A. Persoons, *Phys. Rev. Lett.* **1991**, *66*, 2980.
[35] M. G. Kuzyk, C. W. Dirk (Eds.), *Characterization Techniques and Tabulations for Organic Nonlinear Optical Materials* [in: *Opt. Eng.* (N.Y.), 1998; 60], **1998**.
[36] K. Ruhlandt-Senge, J. J. Ellison, R. J. Wehmschulte, F. Pauer, P. P. Power, *J. Am. Chem. Soc.* **1993**, *115*, 11353.
[37] E. Urnezius, J. D. Protasiewicz, *Main Group Chem.* **1996**, *1*, 369.
[38] M. J. Frisch, G. W. Trucks, H. B. Schlegel, G. E. Scuseria, M. A. Robb, J. R. Cheeseman, J. A. Montgomery Jr., T. Vreven, K. N. Kudin, J. C. Burant, J. M. Millam, S. S. Iyengar, J. Tomasi, V. Barone, B. Mennucci, M. Cossi, G. Scalmani, N. Rega, G. A. Petersson, H. Nakatsuji, M. Hada, M. Ehara, K. Toyota, R. Fukuda, J. Hasegawa, M. Ishida, T. Nakajima, Y. Honda, O. Kitao, H. Nakai, M. Klene, X. Li, J. E. Knox, H. P. Hratchian, J. B. Cross, V. Bakken, C. Adamo, J. Jaramillo, R. Gomperts, R. E. Stratmann, O. Yazyev, A. J. Austin, R. Cammi, C. Pomelli, J. W. Ochterski, P. Y. Ayala, K. Morokuma, G. A. Voth, P. Salvador, J. J. Dannenberg, V. G. Zakrzewski, S. Dapprich, A. D. Daniels, M. C. Strain, O. Farkas, D. K. Malick, A. D. Rabuck, K. Raghavachari, J. B. Foresman, J. V. Ortiz, Q. Cui, A. G. Baboul, S. Clifford, J. Cioslowski, B. B. Stefanov, G. Liu, A. Liashenko, P. Piskorz, I. Komaromi, R. L. Martin, D. J. Fox, T. Keith, M. A. Al-Laham, C. Y. Peng, A. Nanayakkara, M. Challacombe, P. M. W. Gill, B. Johnson, W. Chen, M. W. Wong, C. Gonzalez, J. A. Pople, *Gaussian 03*, Revision C.02, Gaussian, Inc., Wallingford CT, **2004**.
[39] R. Ditchfield, W. J. Hehre, J. A. Pople, *J. Chem. Phys.* **1971**, *54*, 724.
[40] W. J. Hehre, R. Ditchfield, J. A. Pople, *J. Chem. Phys.* **1972**, *56*, 2257.
[41] P. C. Hariharan, J. A. Pople, *Theor. Chim. Acta* **1973**, *28*, 213.
[42] P. C. Hariharan, J. A. Pople, *Mol. Phys.* **1974**, *27*, 209.
[43] M. S. Gordon, *Chem. Phys. Lett.* **1980**, *76*, 163.
[44] M. M. Francl, W. J. Pietro, W. J. Hehre, J. S. Binkley, M. S. Gordon, D. J. DeFrees, J. A. Pople, *J. Chem. Phys.* **1982**, *77*, 3654.
[45] M. Hada, *Phys. Rev. B* **1988**, *37*, 785.
[46] R. C. Binning Jr., L. A. Curtiss, *J. Comput. Chem.* **1990**, *11*, 1206.
[47] A. D. Becke, *J. Chem. Phys.* **1993**, *98*, 5648.
[48] V. A. Rassolov, J. A. Pople, M. A. Ratner, T. L. Windus, *J. Chem. Phys.* **1998**, *109*, 1223.
[49] V. A. Rassolov, M. A. Ratner, J. A. Pople, P. C. Redfern, L. A. Curtiss, *J. Comput. Chem.* **2001**, *22*, 976.
[50] H.-L. Peng, J. L. Payton, J. D. Protasiewicz, M. C. Simpson, *J. Phys. Chem. A* **2009**, *113*, 7054.
[51] M. Chhibber, *Synlett* **2004**, 197.
[52] C.-L. Li, S.-J. Shieh, S.-C. Lin, R.-S. Liu, *Org. Lett.* **2003**, *5*, 1131.

Received: September 2, 2009
Published Online: January 12, 2010

